Electronic Supplementary Material (ESI) for Lab on a Chip.

Suppl. Figures

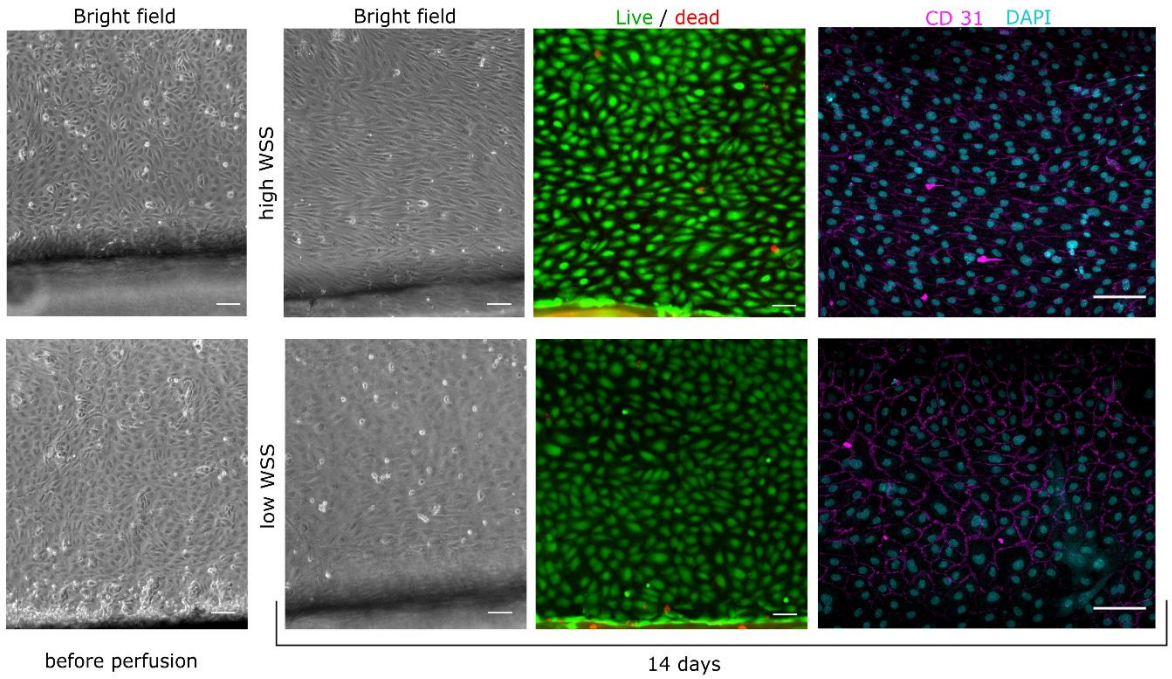

Suppl. Fig. 1: Long-term culture of HUVEC in the perfusion channels of the rOoC under high and low WSS. Representative Bright-field images, live-dead, and immunofluorescence staining.

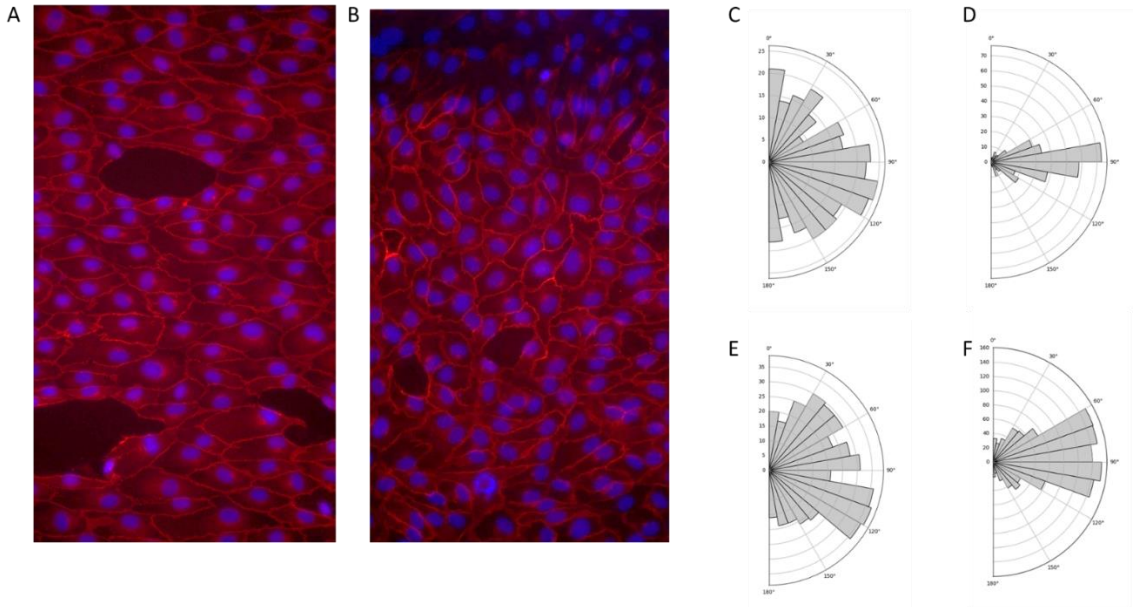

Suppl. Fig. 2: Alignment of HUVEC cells under different flow regimes: A/B) Fluorescence image of HUVEC cells cultivated in the perfusion channels (red: Actin, blue: Nuclei) in the outer channel (A) and the inner channel (B). C/D: Alignment histogram of nuclei for high flow rate – inner (C) and outer (D) channel. E/F: Alignment histogram of nuclei for low flow rate – inner (E) and outer (F) channel

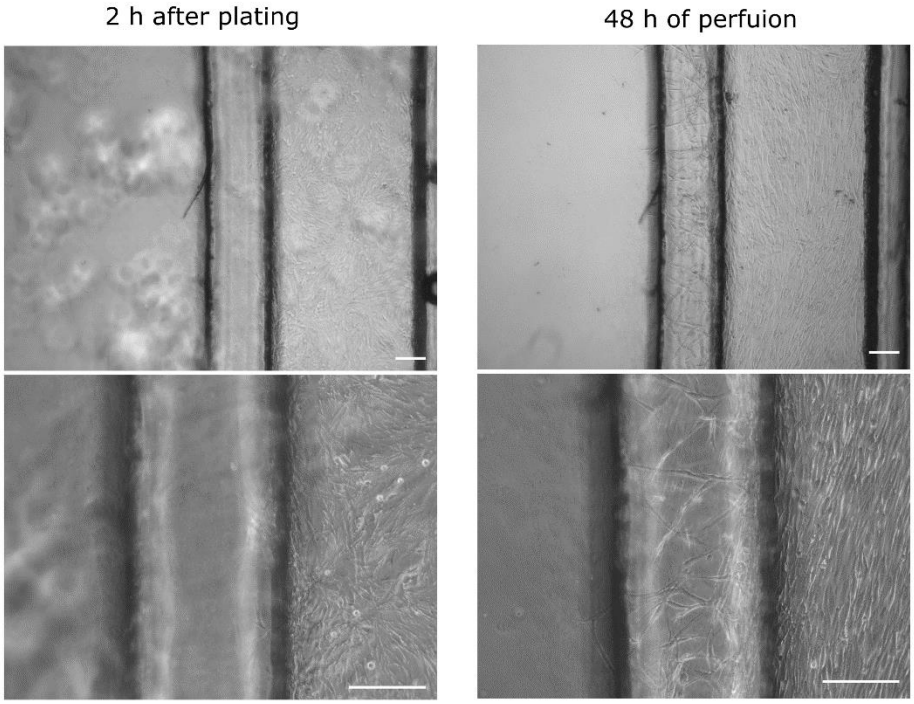

Suppl. Fig. 3: Human liver endothelial cells (HLEC) in the rOoC. Representative bright field images show alignment in the perfusion channel and sprouting toward the organoid compartment of HLEC after 48 h of perfusion.

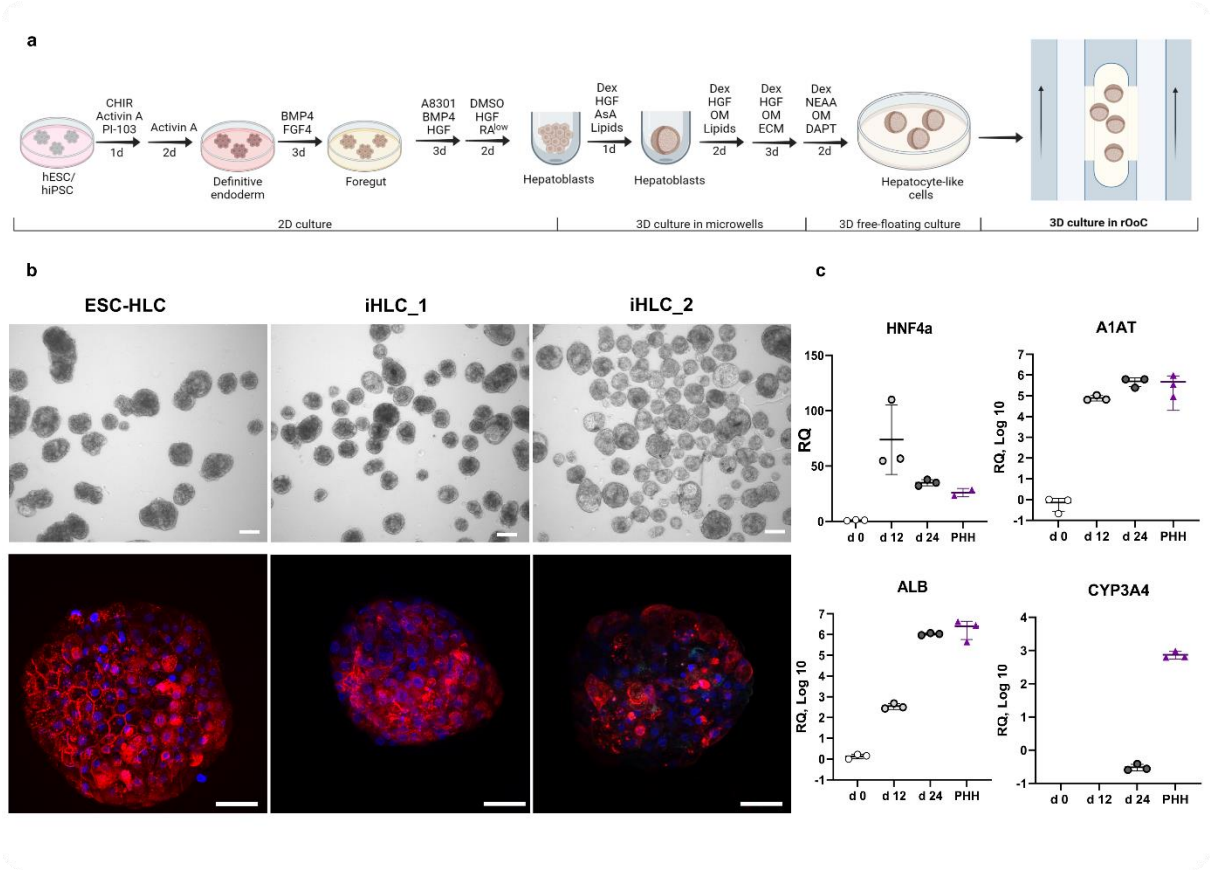

Suppl. Fig. 4 Differentiation and characterization of embryonic stem cell (ESC) and iPSC-derived human liver cell (HLC) organoids. a) Schematic representation of the used differentiation protocol. b) Representative bright field (upper row) and immunofluorescence (lower row) images of HLC organoids generated from human ESC and iPSC lines. Red – albumin, Blue – nuclei. Scale bar 50 µm. c) Relative expression of selected hepatic markers for three different SC-derived HLC organoids (d 0, d 12, and d 24 of differentiation) compared with primary hepatic organoids (PHH) for n = 3 donors.

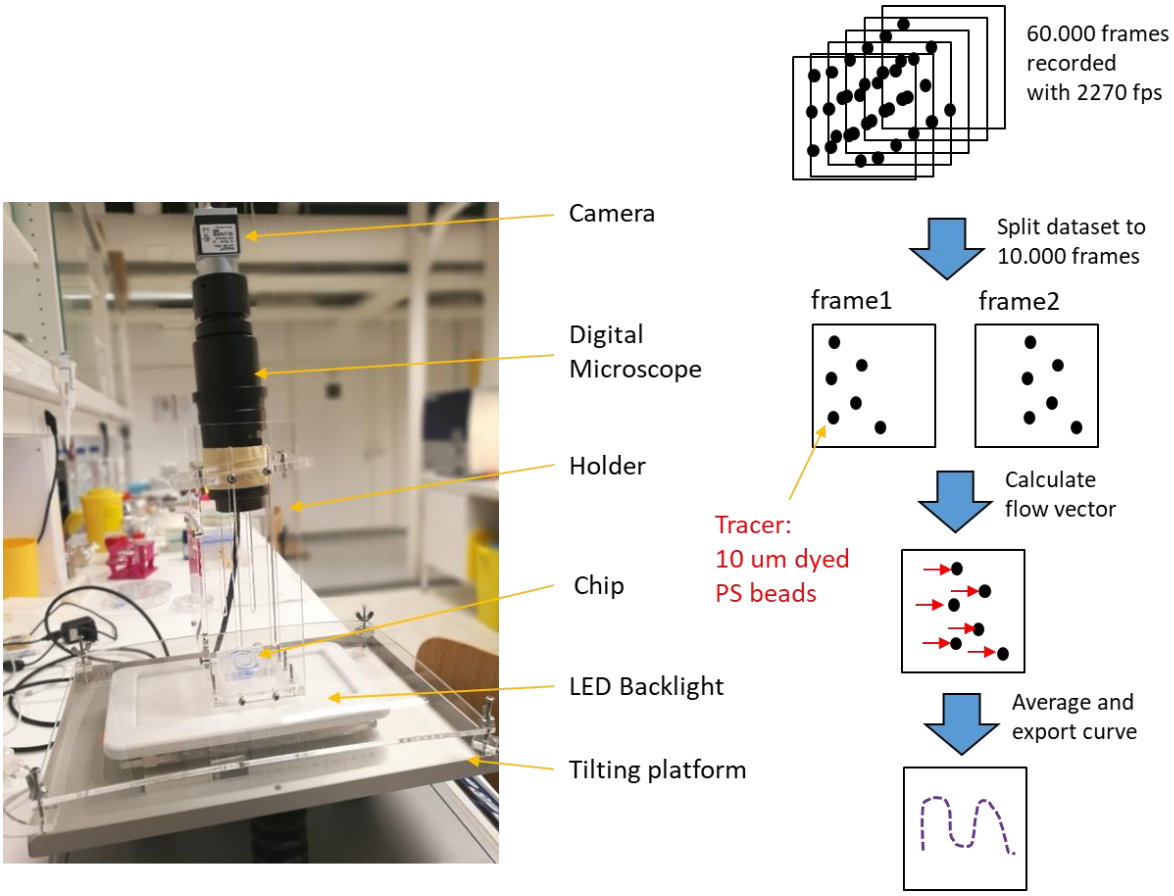

Suppl. Fig. 5: Optical setup and toolchain for micro-particle-image velocimetry (µPIV) analysis used in this study.

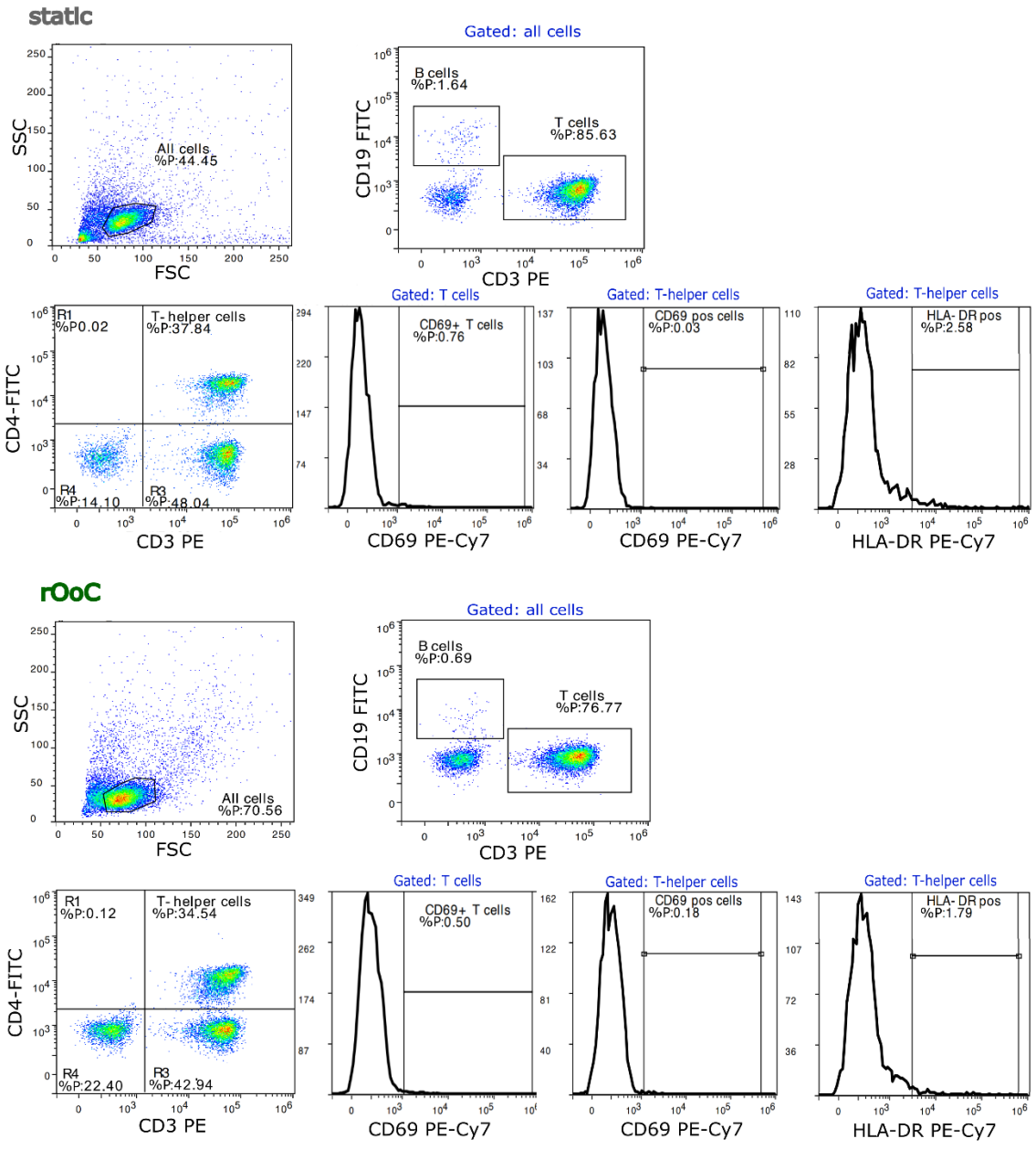

Suppl. Fig. 6: Gating strategy for human PBMCs. Representative dot blots showing the gating strategy for identifying B cells, T cells, and T-helper cells by flow cytometry. Representative histograms show the percentage of activated T- and T-helper cells under static and fluidic conditions (rOoC) after 24 h. Flow cytometry experiments were replicated for 3 healthy donors.

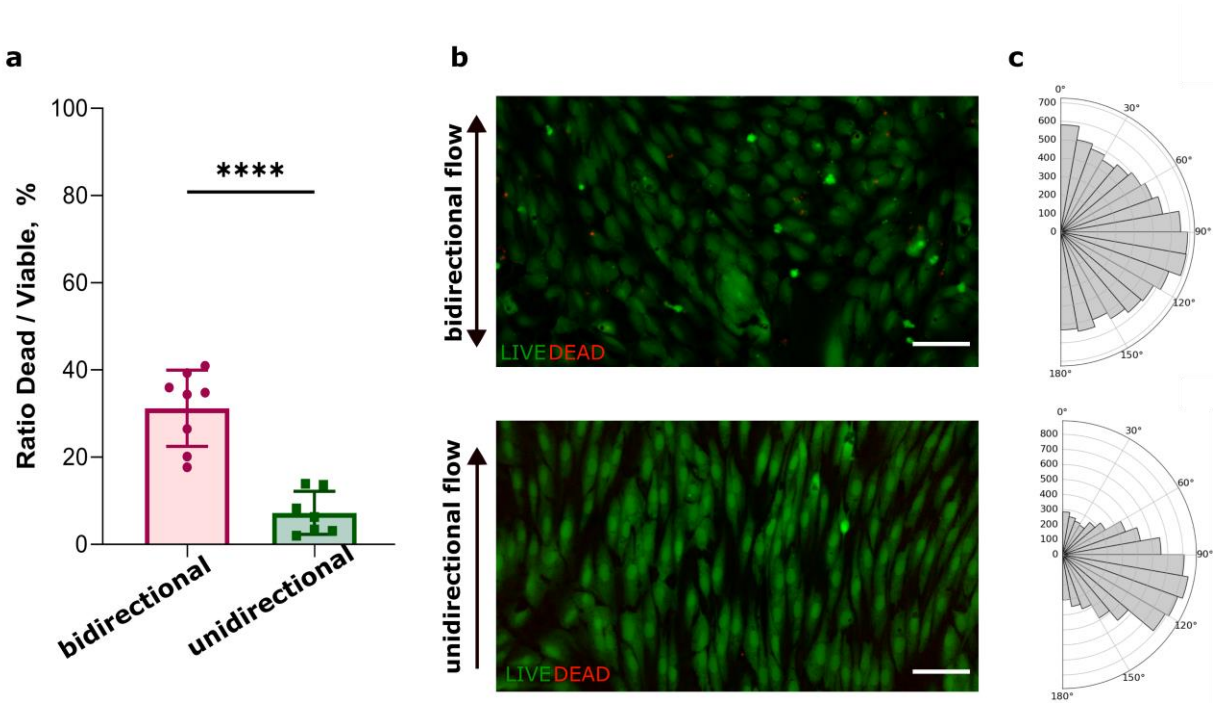

Suppl. Fig. 7: Comparison of HUVEC culture under bi- vs unidirectional flow stimulation: a) Viability of HUVECS after 48h of cultivation under unidirectional and bidirectional flow conditions. The ratio of dead/live cells was calculated from 8/7 images each (2 independent chips for each conditions). Comparison is performed by unpaired t-test; data is represented as mean +/- SD. b) Fluorescence image of living (green) and dead (red) cells under both conditions. Scale bar is 50µm. c) Histogram plot of cell alignment for both conditions (as cell count in each bin). The same dataset as in a) is used.

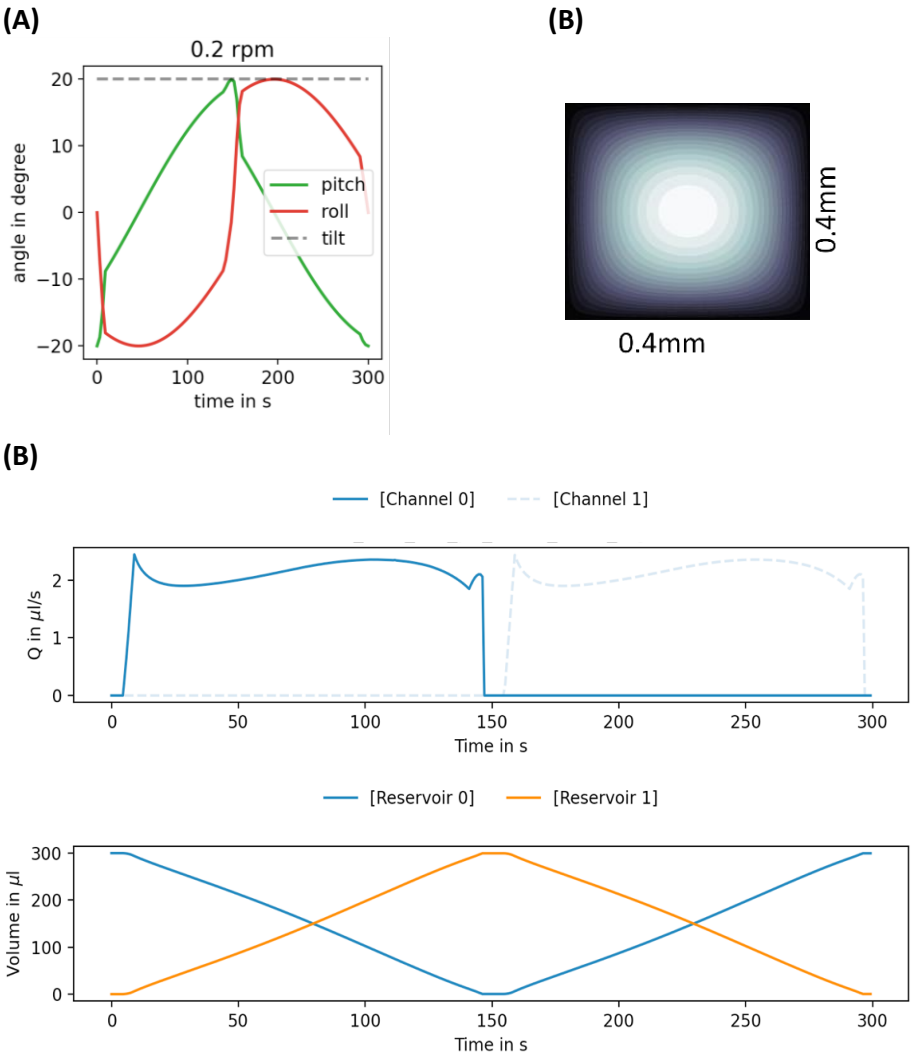

Suppl. Fig. 8: Predictive modeling for alternative actuation patterns: (A) Pitch and roll of the rotation platform for 0.2-rpm speed and a not-symmetric speed profile. (B) Reduced channel dimensions with cross-sectional area of 0.4 x 0.4 mm2 (aspect ratio 1.0) caused reduced flow rates. The outer reservoir was filled with 300µl initially and µ=0.8 mPa s. The maximal Reynolds number was 6.2, and the maximum wall shear stress was 2.4 dyne/cm2. (B) Channel flow rates (outer channel) and (outer) reservoir volumes are shown over time. Virtually constant channel flow rates over several minutes can be achieved with non-uniform rotation sequences and low transmissibility channels.